

## Sound Emission due to Superfluid Vortex Reconnections

M. Leadbeater,<sup>1</sup> T. Winiecki,<sup>1</sup> D. C. Samuels,<sup>2</sup> C. F. Barenghi,<sup>2,3</sup> and C. S. Adams<sup>1</sup>

<sup>1</sup>*Department of Physics, University of Durham, Durham DH1 3LE, United Kingdom*

<sup>2</sup>*Department of Mathematics, University of Newcastle, Newcastle NE1 7RU, United Kingdom*

<sup>3</sup>*Isaac Newton Institute for Mathematical Sciences, University of Cambridge, Cambridge CB3 0EH, United Kingdom*

(Received 5 September 2000)

By performing numerical simulations based on the Gross-Pitaevskii equation, we make direct quantitative measurements of the sound energy released due to superfluid vortex reconnections. We show that the energy radiated expressed in terms of the loss of vortex line length is a simple function of the reconnection angle. In addition, we study the temporal and spatial distribution of the radiation and show that energy is emitted in the form of a sound pulse with a wavelength of a few healing lengths.

DOI: 10.1103/PhysRevLett.86.1410

PACS numbers: 03.75.Fi, 67.40.Vs, 67.57.De

The decay of superfluid turbulence in the limit of low temperature raises some fundamental questions in the field of quantum fluids. For example, vortex tangles produced in superfluid helium at  $T < 100$  mK are observed to decay [1], but at these temperatures the frictional dissipation due to thermal excitations is practically negligible. Recent theoretical work [2–4] has highlighted the possible role of sound emission as a dissipation mechanism. Sound emission may occur due to vortex motion or reconnection; however, conventional numerical simulations based on vortex filaments governed by incompressible Euler dynamics (the Biot-Savart law) are unable to describe this process. A useful tool to study vortex-sound interactions is the Gross-Pitaevskii (GP) equation. Although unable to fully represent the physics of HeII, the GP equation does provide a sophisticated fluid dynamical model capable of describing vortex nucleation [5] and reconnections [6–8]. Furthermore, the GP equation has been shown to provide an accurate description of the recently discovered atomic Bose-Einstein condensates [9], where similar issues of vortex-sound interactions are likely to occur, particularly in experiments where many vortices are formed [10,11].

In this Letter, we compute the sound energy radiated due to superfluid vortex reconnections using the GP model. We parametrize the energy in terms of vortex line length, and show that the vortex line length destroyed during a reconnection is a simple function of the reconnection angle. In addition, we measure the temporal and spatial distributions of the radiation and show that energy is emitted in the form of a rarefaction pulse which subsequently disperses into sound waves.

To create a reconnection we collide two vortex rings with radius  $R$  whose axes of propagation are offset by a distance  $D$ . This system has the advantage that a well-behaved initial state can be constructed within a spatially confined region, and the reconnection occurs “naturally” due to the self-induced motion of the vortex rings. In addition, by varying the offset we can study a range of reconnection angles,  $\theta$ , where we define  $\theta = 2 \cos^{-1}(D/2R)$ . We adopt the same numerical methods as in our previous papers [12–14]. The key points are that throughout the

paper we use dimensionless units, where distance and velocity are measured in terms of the healing length  $\zeta$  and the sound speed  $c$ , respectively. In addition, the asymptotic number density  $n_0$  is rescaled to unity. The initial state is taken as the product of two vortex ring states,  $\psi(\mathbf{r}, 0) = \phi_1(\mathbf{r} - \mathbf{r}_1)\phi_2^*(\mathbf{r} - \mathbf{r}_2)$ , where  $\phi_{1,2}(\mathbf{r})$  are time-independent vortex ring solutions of the uniform flow equation found by Newton’s method [13]. We arrange for the rings to propagate in the  $\pm x$  directions with an offset in the  $y$  direction, i.e.,  $\mathbf{r}_{1,2} = (\pm 25v, \pm D/2, 0)$ , where  $x$ ,  $y$ , and  $z$  correspond to the axes shown in Fig. 1,  $v$  is the ring velocity, and  $D$  is the offset between the propagation axes of the two rings. The initial state is evolved according to the dimensionless GP equation,

$$i\partial_t\psi = -\frac{1}{2}\nabla^2\psi + (|\psi|^2 - 1)\psi, \quad (1)$$

using a semi-implicit Crank-Nicholson algorithm. To model a large box, we map an infinite length onto the space  $-1 \leq x' \leq 1$  using  $x' = x/(|x| + \zeta)$  with  $\zeta = 12$ . We use a grid spacing,  $\Delta x' = 0.014$ , and a time step,  $\Delta t = 0.01$ . Simulations have been performed with vortex ring radii of  $R = 5.04, 6.00, \text{ and } 7.30$ , which correspond to velocities  $v = 0.34, 0.3, \text{ and } 0.26$ , respectively. The range of  $R$  is limited by numerics; smaller rings are too fast to resolve the sound pulse, and larger rings require more grid points.

A typical sequence illustrating the vortex ring collision is shown in Fig. 1. As the rings approach they stretch in the  $yz$  plane. The reconnections occur along the  $z$  axis at about  $t = 30$ . The reconnections produce two highly elongated rings and two sound pulses which propagate outwards along the  $\pm z$  axis. The sound pulse appears in Fig. 1 as an oval in the centre of the top view at  $t = 40$ . The stretched rings ( $t = 50$ ) rapidly shrink into two smaller vibrating rings which move outwards. For the offset  $D = 4$  shown in Fig. 1, the outgoing rings propagate at an angle  $\phi = \pm 56^\circ$  to the  $x$  axis. The smaller radius of the outgoing rings reflects the energy loss due to the reconnections. For larger offsets, the collision is less violent than the

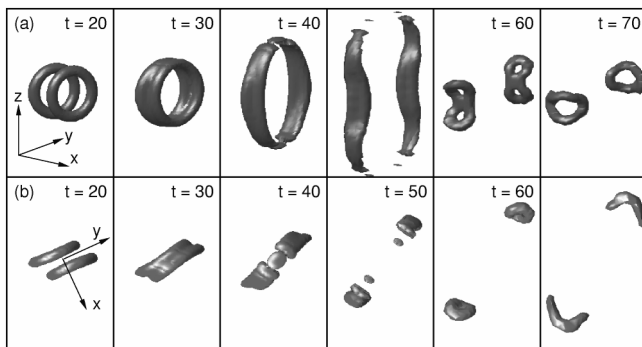


FIG. 1. Sequence of density isosurfaces ( $|\psi|^2 = 0.75$ ) illustrating a vortex ring collision with ring radius  $R = 6$  and offset  $D = 4$ . A side view (a) and a top view (b) are shown. Initially, the rings propagate along the  $x$  axis and collide in the  $yz$  plane at  $t \sim 30$ . The collision produces highly stretched rings ( $t = 50$ ) which snap back into two smaller rings moving at  $\pm 56^\circ$  to the  $x$  axis. The sound pulse is emitted along the  $\pm z$  axis, and appears as an oval in the centre of the top view at  $t = 40$ .

example shown, and the scattering angle of the outgoing rings  $\phi$  is smaller.

To quantify the sound energy we calculate the energy within a measurement sphere of radius 20. The energy is defined relative to a uniform laminar state as in our previous work [13]. The energy per ring as a function of time for collisions between rings with radii  $R = 6.0$ , offset by  $D = 2$  to  $D = 8.5$ , is shown in Fig. 2 (inset). If the reconnection occurs a few healing lengths along the  $z$  axis at  $t \sim 30$ , and the sound pulse travels outwards at speed  $c = 1$ , then one would expect to observe the sound leaving the measurement volume between  $t = 45$  and  $t = 50$ . This appears as an energy drop in the numerical data [Fig. 2 (inset)]. After the sound pulse has left the sphere one expects the energy to remain approximately constant until the outgoing vortex rings leave between  $t = 60$  and  $t = 75$ . This energy “plateau” is well defined in Fig. 2 (inset) for offsets between  $D = 4$  and  $D = 8.5$ , but for smaller offsets the outgoing rings are too fast to be resolved from the sound pulse. We define the radiated sound energy as the difference between the initial energy and the value at the center of the plateau. Note that for  $D \sim R/2$  ( $\theta \sim \pi/2$ ) a second plateau is observed. This corresponds to sound energy emitted inwards which has farther to travel and therefore leaves the measurement volume later.

In general, the energy loss will depend on the particular configuration of vortex lines. For this reason, a better approach may be to determine the change in the vortex line length. To convert between energy and length, we define the energy of a vortex ring with radius  $R$  as [15]

$$E = 2\pi^2 R \left[ \ln\left(\frac{8R}{a}\right) - 1.615 \right], \quad (2)$$

with  $a = 1/\sqrt{2}$ . This is an approximation as the outgoing vortex rings are excited. The vortex line length destroyed,  $l_{\text{loss}}$ , as a function of reconnection angle,  $\theta = 2 \cos^{-1}(D/2R)$ , is plotted in Fig. 2. For intermediate angles, the data lie on a unique curve independent of  $R$ ,

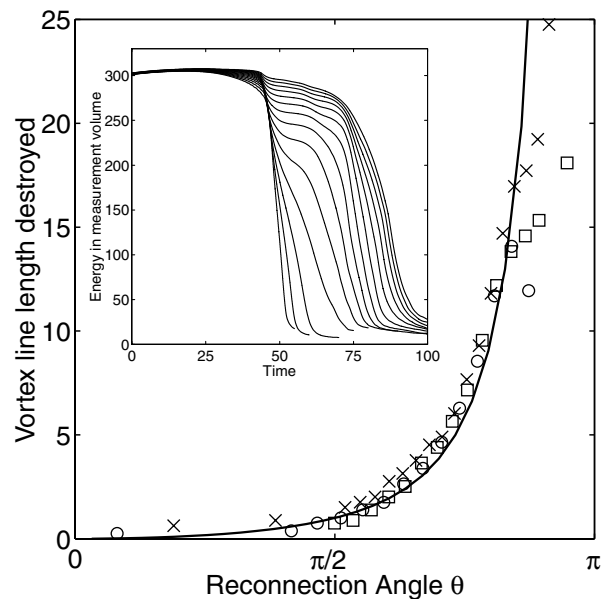


FIG. 2. Vortex line length destroyed,  $l_{\text{loss}}$  (in units of the healing length), as a function of the reconnection angle  $\theta$ . The line shows  $l_{\text{loss}} = \tan^2(\theta/2)$ . The numerical data are for ring radii of  $R = 5.04$  ( $\circ$ ),  $6.00$  ( $\square$ ), and  $7.30$  ( $\times$ ), and offsets  $D$  from  $2R$  to  $0$ , corresponding to  $\theta$  from  $0$  to  $\pi$ . The vortex line length destroyed is determined from the energy decrease within a measurement sphere when the sound pulse exits. The time dependence of the energy per ring within the measurement sphere for ring radius  $R = 6.0$  and offsets  $D = 2-8.5$  in increments of  $0.5$  is shown in the inset. The sound energy exits between  $t = 48$  and  $t = 52$ . The energy plateau at  $t \sim 60$  indicates the energy loss due to sound emission. This second plateau visible for  $D \sim R$  corresponds to the sound energy emitted inwards.

which justifies the choice of vortex line length for the analysis. A reasonable fit is given by,  $l_{\text{loss}} \sim \tan^2(\theta/2) = (4R^2 - D^2)/D^2$ , where  $l_{\text{loss}}$  is measured in units of the healing length. A  $\theta$  dependence of this form may arise because the initial curvature, and hence the acceleration of the vortex line, is proportional to  $\tan(\theta/2)$ . If one models the sound emission as a frictional drag force [16], then the energy emitted (or the vortex line lost) is proportional to the square of the acceleration, i.e.,  $\tan^2(\theta/2)$ . The characteristic length scale for the vortex line loss must be related to the vortex core size. Our simulations suggest that this length is of the order of the healing length  $\xi$ .

Numerical errors are expected at small and large  $\theta$ : First, for large  $\theta$  (small offset  $D$ ), most of the energy is emitted as sound, and the energy plateau is not well defined leading to a large error. Second, an error occurs when comparing Eq. (2) with our numerical energy data due to the finite size of the measurement volume. This error is largest when the incoming and outgoing rings are largest, i.e., for large  $R$  and large  $D$ . This leads to the overestimate of vortex line loss apparent for the  $R = 7.30$ ,  $\theta < \pi/2$  data in Fig. 2.

The dependence of the vortex line loss on reconnection angle can, in principle, be applied to determine the sound energy emitted in other reconnection geometries. In the case of straight line vortices, it is known that the lines

tend to become more antiparallel as they approach [17,18]. This effect appears as a stretching of the vortex rings in our simulation (see Fig. 1), and may partly account for the rapid increase in the energy loss for  $\theta > \pi/2$ . To include this effect in a model of superfluid turbulence,  $\theta$  should be taken as the initial angle between the vortex lines before it is altered by their proximity.

To convert the dimensionless units into values applicable to HeII, we take the number density as  $n_0 = 2.18 \times 10^{28} \text{ m}^{-3}$ , the quantum of circulation as  $\kappa = h/m = 9.98 \times 10^{-8} \text{ m}^2 \text{ s}^{-1}$ , and the healing length as  $\xi/\sqrt{2} = 0.128 \text{ nm}$  [19]. The unit of energy is then  $\hbar n_0 c \xi^2 = 6.56 \times 10^{-24} \text{ J}$  or 0.475 K. For these parameters, the energy radiated for reconnection angles of  $\pi/2$  and  $3\pi/4$  are  $9.2 \times 10^{-23} \text{ J}$  (6.65 K) and  $5.2 \times 10^{-22} \text{ J}$  (37.5 K), respectively.

To determine the character of the sound radiation we have studied the temporal and spatial distribution of the emission. The density along the  $z$  axis for a collision with ring radius  $R = 6$  and offset  $D = 8$  is shown in Fig. 3. Initially the density is uniform, except for a slight increase near the origin indicating the approaching rings. Between  $t = 25$  and  $t = 30$  the rings collide in the  $xy$  plane. During the collision, the vortex cores merge while the rings grow outwards. Because of this stretching effect, the reconnection point is pushed outwards along the

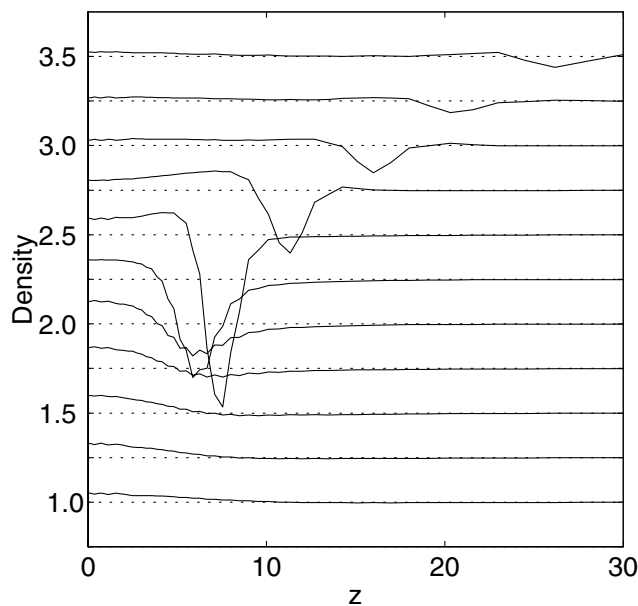


FIG. 3. The density along the  $z$  axis for a collision between two vortex rings with radius  $R = 6$  and offset  $D = 8$ . The eleven curves, corresponding to times  $t = 0$  to  $t = 50$  in increments of 5, are offset in increments of 0.25 along the  $y$  axis. Initially the density is uniform except for a slight increase near the origin indicating the approaching rings. Between  $t = 25$  and  $t = 30$  the rings collide in the  $xy$  plane. This results in the formation of a rarefaction pulse which moves outwards. Note that initially the density at the center of the rarefaction pulse is zero and then increases. For  $t > 40$  the pulse evolves into a sound wave with a wavelength of 6–8 healing lengths.

$z$  axis to  $z \sim \pm 7$  and delayed until  $t \sim 29$  (if there were no distortion of the incoming rings, one would expect the reconnection to occur at  $z = \pm 4.5$  and  $t = 25$ ). When the circulation is cancelled at  $t = 29$ , the density is zero at  $z = \pm 7$ . This density minimum continues to move outwards in the same direction as the vortex cores prior to the reconnection. As the pulse moves outwards the density minimum gradually fills in.

As shown for the case of vortex nucleation by a moving sphere [14], further insight can be gained by considering the time evolution as a transition between time-independent states. For the head-on collision ( $D = 0$ ), one can regard the segments of the ring as antiparallel vortex lines. The two-dimensional time-independent solutions for two opposite sign vortices have been studied by Jones and Roberts [20]. They show that when the vortex cores merge they form a rarefaction pulse. In a three-dimensional situation, as the rarefaction pulse expands outwards, the energy per unit length decreases which corresponds to a lower energy on the dispersion curve. The lower energy rarefaction pulse has a higher central density and moves faster, eventually approaching the sound speed [20]. This exactly describes the behavior apparent in Fig. 3. Eventually the rarefaction pulse evolves into a sound wave with a central wavelength of approximately seven healing lengths. For HeII, taking  $\xi/\sqrt{2} = 0.128 \text{ nm}$  [19], this converts to 1.3 nm,

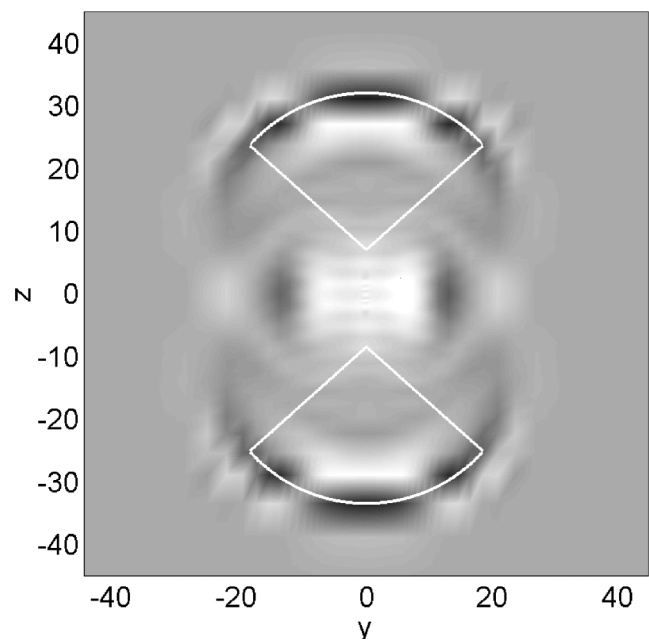


FIG. 4. Density cross-sections in the  $x = 0$  plane at  $t = 54$  for ring radii  $R = 6$  with offset  $D = 8$  (same parameters as in Fig. 3). The sound pulse appears as two arcs with radius of curvature, 25, suggesting that the reconnections occurred at  $z = \pm 7$  and  $t = 29$ , consistent with Fig. 3. The angular spread is approximately equal to the reconnection angle ( $\theta = 96^\circ$  for this example). The white lines indicate the positions of the reconnections,  $z = \pm 7$ , the reconnection angle  $\theta$  and the expected position of the sound pulse. Grey scale: black 0.95; white 1.025.

which corresponds to an intermediate phonon wavelength (cf. maxon and roton wavelengths of 0.6 and 0.3 nm, respectively).

The spatial extent of the sound pulse in the  $x = 0$  plane, for the same parameters as in Fig. 3 but at a later time,  $t = 54$ , is shown in Fig. 4. The vortex rings have moved out of the  $yz$  plane by  $t = 54$ , as in the example shown in Fig. 1. The main component of the sound pulse appears as two crescent-shaped density waves traveling outwards with an angular distribution roughly equal to the reconnection angle (indicated by the white lines in Fig. 4). The weaker density wave emitted inwards accounts for the second plateau in the energy curves shown in Fig. 2 (inset). A similar distribution is observed in the  $y = 0$  plane. By  $t = 54$ , the sound energy is spread over a large area and the amplitude of the density variation is very small (only a few percent). The spherical wave fronts are consistent with the reconnection position and time indicated by Fig. 3.

In summary, we have made direct quantitative measurements of the sound energy emitted due to superfluid vortex reconnections. We show that the energy radiated leads to a loss of vortex line length which is a simple function of the reconnection angle. The energy radiated increases dramatically as the lines become more antiparallel which suggests that reconnections may be a significant decay mechanism for superfluid turbulence in the limit of low temperature. We also show that the radiation initially appears in the form of a rarefaction pulse which evolves into a sound wave with a wavelength of a few healing lengths.

We thank the Newton Institute, Cambridge University, where part of this work was completed. Financial support was provided by the EPSRC.

- [1] P. C. Hendry, N. S. Lawson, R. A. M. Lee, and P. V. E. McClintock, *Nature (London)* **368**, 315 (1994).
- [2] C. Nore, M. Abid, and M. E. Brachet, *Phys. Rev. Lett.* **78**, 3896 (1997).
- [3] D. C. Samuels and C. F. Barenghi, *Phys. Rev. Lett.* **81**, 4381 (1998).
- [4] W. F. Vinen, *Phys. Rev. B* **61**, 1410 (2000).
- [5] T. Frisch, Y. Pomeau, and S. Rica, *Phys. Rev. Lett.* **69**, 1644 (1992).
- [6] J. Koplik and H. Levine, *Phys. Rev. Lett.* **71**, 1375 (1993).
- [7] J. Koplik and H. Levine, *Phys. Rev. Lett.* **76**, 4745 (1996).
- [8] M. Tsubota, S. Ogawa, and Y. Hattori (to be published).
- [9] See, e.g., *Bose-Einstein Condensation in Atomic Gases: Proceedings of the International School of Physics "Enrico Fermi,"* edited by M. Inguscio, S. Stringari, and C. Wieman (IOS Press, Amsterdam, 1999).
- [10] C. Raman, M. Köhl, R. Onofrio, D. S. Durfee, C. E. Kulewicz, Z. Hadzibabic, and W. Ketterle, *Phys. Rev. Lett.* **83**, 2502 (1999).
- [11] K. W. Madison, F. Chevy, W. Wohlleben, and J. Dalibard, *J. Mod. Opt.* **47**, 2715 (2000).
- [12] T. Winiecki, J. F. McCann, and C. S. Adams, *Phys. Rev. Lett.* **82**, 5186 (1999).
- [13] T. Winiecki, J. F. McCann, and C. S. Adams, *Europhys. Lett.* **48**, 475 (1999).
- [14] T. Winiecki and C. S. Adams, *Europhys. Lett.* **52**, 257 (2000).
- [15] P. H. Roberts and J. Grant, *J. Phys. A* **4**, 55 (1971).
- [16] R. A. Ferrell, *J. Low Temp. Phys.* **119**, 257 (2000).
- [17] K. W. Schwarz, *Phys. Rev. B* **31**, 5782 (1985).
- [18] A. T. A. M. DeWaele and R. G. K. M. Aarts, *Phys. Rev. Lett.* **72**, 482 (1994).
- [19] G. W. Rayfield and F. Reif, *Phys. Rev.* **136**, 1194 (1964).
- [20] C. A. Jones and P. H. Roberts, *J. Phys. A* **15**, 2599 (1982).